On the response of HALOE stratospheric ozone and temperature to the 11-yr solar cycle forcing

E. E. Remsberg[1]

[1]Science Directorate, NASA Langley Research Center, Hampton, VA

E. E. Remsberg, Science Directorate, Mail Stop 401B, NASA Langley Research Center, Hampton, VA 23681-2199. (e-mail: Ellis.E.Remsberg@nasa.gov)

Abstract.

Results are presented on responses in 14-yr time series of stratospheric ozone and temperature from the Halogen Occultation Experiment (HALOE) of the Upper Atmosphere Research Satellite (UARS) to a solar cycle (SC-like) variation. The ozone time series are for ten, 20-degree wide, latitude bins from 45S to 45N and for thirteen "half-Umkehr" layers of about 2.5 km thickness and extending from 63 hPa to 0.7 hPa. The temperature time series analyses were restricted to pressure levels in the range of 2 hPa to 0.7 hPa. Multiple linear regression (MLR) techniques were applied to each of the 130 time series of zonally-averaged, sunrise plus sunset ozone points over that latitude/pressure domain. A simple, 11-yr periodic term and a linear trend term were added to the final MLR models after their seasonal and interannual terms had been determined. Where the amplitudes of the 11-yr terms were significant, they were in-phase with those of the more standard proxies for the solar uv-flux. The max minus min response for ozone is of order 2 to 3% from about 2 to 5 hPa and for the latitudes of 45S to 45N. There is also a significant max minus min response of order 1 K for temperature between 15S and 15N and from 2 to 0.7 hPa. The associated linear trends for ozone are near zero in the upper stratosphere. Negative ozone trends of 4 to 6%/decade were found at 10 to 20 hPa across the low to middle latitudes of both hemispheres. It is concluded that the analyzed responses from the HALOE data are of good quality and can be used to evaluate the responses of climate/chemistry models to a solar cycle forcing.

1. Introduction

There have been a number of model studies focused on the response of middle atmosphere ozone to the 11-yr cycle of the solar ultraviolet (uv)-flux forcing (e.g., *Garcia et al.,* 1984; *Brasseur,* 1993; *Huang and Brasseur*, 1993; *Fleming et al.,* 1995; *Harris et al.,* 1998; *Shindell et al.,* 1999; *Callis et al.,* 2000; *Lee and Smith*, 2003; *Marsh et al.,* 2003; *Rozanov et al.*, 2004; *Austin et al.,* 2007; *Marsh et al.*, 2007; *McCormack et al.,* 2007; *Nissen et al.,* 2007; *Smith and Matthes*, 2008; *Austin et al.,* 2008). It is important to verify those modeled responses as a function of altitude, latitude, and season using high quality, global-scale observations of ozone. Analyses of the long-term satellite ozone data sets from the Stratospheric Aerosol and Gas Experiments (SAGE I/II) and from the series of Solar Backscatter Ultra-Violet (SBUV) instruments have yielded zonal-mean solar-cycle (SC) response patterns having maxima at middle latitudes from about 3 to 1.5 hPa (or ~40 to 45 km) [e.g., *Wang et al.,* 1996; *Chandra and McPeters,* 1994; *McCormack and Hood*, 1996; *Lee and Smith*, 2003; *Soukharev and Hood,* 2006; *Randel and Wu*, 2007]. However, the patterns for those responses do not agree so well with many of the simulations, which tend to peak at somewhat lower altitudes and lower latitudes. In addition, the SC amplitudes derived from the observations are about twice those from many of the models. On the other hand, *Chandra and McPeters* [1994] reported very good agreement between modeled and observed responses to the uv-flux variations associated with the 27-day solar rotation cycle.

Wang et al. [1996] found that the apparent SC response in the SAGE dataset was larger and occurred at higher latitudes for the northern hemisphere (NH) than for the southern

58 hemisphere (SH). Conversely, *Lee and Smith* [2003] found a SC response in the SBUV
59 data that was larger in the SH, but they also cautioned that the observed responses may
60 depend on the specific decade(s) for the given datasets. Those apparent differences have
61 led researchers to consider the role of decadal-scale dynamical interactions for ozone,
62 particularly for the middle and lower stratosphere [*Nedoluha et al.,* 1998; *Randel et al.,*
63 2000; *Tian et al.,* 2006; *McCormack et al.*, 2007; *Smith and Matthes*, 2008]. Such
64 considerations have prompted further model studies that include the effects of
65 atmospheric interactions with the semi-annual oscillation (SAO) and quasi-biennial
66 oscillation (QBO) cycles, as well as influences from volcanic events and from the El
67 Nino/Southern Oscillation (ENSO). All of these forcings could alter a decadal-scale
68 ozone response, perhaps even having a maximum that is in-phase with the SC for the
69 stratosphere but located at middle latitudes rather than at tropical latitudes—or more like
70 those obtained from the preceding data analysis studies [e.g., *Matthes et al.,* 2004; *Lee*
71 *and Smith,* 2003; *Kodera and Kuroda,* 2002]. *Hood* [2004] summarized the nature of the
72 model/data discrepancies for the 11-yr SC response.
73
74 A proper characterization of the SC response in ozone is also critical to a search for a
75 slowdown for the decline of ozone during the 1990s and/or for its recovery since then, in
76 association with the effects of the mandated reductions for the release of
77 chlorofluorocarbon compounds into the atmosphere [*Reinsel,* 2002; *Reinsel et al.,* 2002;
78 *Newchurch et al.,* 2003; *Steinbrecht et al.,* 2004a; *Cunnold et al.,* 2004; *Steinbrecht et al.,*
79 2004b; *Weatherhead et al.,* 1998; *Randel and Wu*, 2007]. For example, *Anderson and*
80 *Russell* [2004] and *WMO* [2007, Figure 1-12] report that the total chlorine derived from

81 measurements of HCl obtained with the Halogen Occultation Experiment (HALOE)
82 leveled-off after about 1997 and began to decline after 2001. Thus, it is reasonable that
83 the trends for upper stratospheric ozone have been changing due to its chemical
84 interactions, too [*Siskind et al.,* 1998]. *Rosenfield et al.* [2005] reported that the chemical
85 response of ozone ought to be asymmetric between the northern and southern
86 hemispheres because of their differences for the distributions of the species responsible
87 for ozone loss.
88
89 A proper characterization of the solar cycle or any other decadal-scale variation is also
90 important for the determination of the ozone trend. For example, *Soukharev and Hood*
91 [2006] analyzed for interannual, SC and trend effects, as part of their regression modeling
92 of the SBUV, SAGE II, and HALOE ozone datasets. They focused primarily on the SC
93 terms from their regression modeling, although they did show that the SC terms that they
94 obtained from the SBUV dataset had response profiles at low latitudes that were similar
95 for 1979-1991 and from 1992-2003—decadal periods when the trends in upper
96 stratosphere ozone were quite different.
97
98 Another important aspect of the fidelity of the observed SC response in ozone is how it
99 relates to the SC response in temperature versus pressure, or T(p). Up until recently, that
100 response in temperature had been obtained only with data from the NOAA operational
101 sounding instruments, which provide relatively low vertical resolution radiance profiles
102 for its retrieval in the stratosphere. Three distinct versions of the T(p) derived from the
103 radiance data lead to SC responses that have a maximum at low latitudes, but which have

104 different magnitudes and are occurring over a different range of pressure-altitudes
105 [*McCormack and Hood,* 1996; *Scaife et al.,* 2000; *Crooks and Gray*, 2005]. There is also
106 a problem with the drifting local time of the NOAA instruments, which could introduce
107 long-term temperature variations because different times of the daily temperature cycle
108 are sampled [*Shine et al.,* 2008]. As a result, there is some uncertainty about which T(p)
109 dataset is more appropriate for comparison with the observed SC ozone responses.
110
111 This paper contains results of analyses for the decadal-scale responses and trends in
112 ozone and T(p) based on data for 1991-2005 from the single, well-calibrated HALOE
113 instrument. In particular, it is focused on the characterization of the response of its upper
114 stratospheric ozone and temperature to the 11-yr SC, keeping in mind that the HALOE
115 measurements span only one complete SC. For this reason the results herein may be
116 considered somewhat exploratory, rather than definitive. Because the trends in upper
117 stratospheric ozone due to its interaction with chlorine were small during the time span of
118 the HALOE measurements [*Rosenfield et al.,* 2005; *Yang et al.,* 2006], it was felt that one
119 could have better success with isolating a SC-like response for the time period of
120 HALOE rather than for the datasets that included the 1980s, too. Also different from the
121 two previous solar maxima, there was no interference from a volcanic eruption near the
122 solar maximum of 2001 [*Solomon et al*, 1996]. Because the calculated percentage SC-
123 like response in ozone is much larger than its percentage response in T(p) it ought to be
124 easier to isolate an SC-like signal in ozone. Nevertheless, one must still be aware that it
125 is easy to confound the effects of a SC term and a trend term, especially when adjacent

126 points in the time series of the zonal means are correlated, and/or when the end portions
127 of the time series are anomalous (e.g., *Tiao et al.* [1990]).
128
129 Section 2 reviews the attributes of the HALOE ozone profiles, along with the time series
130 approach to their analysis. Section 3 includes the findings from those analyses and
131 describes the important similarities and differences with the SC responses from the
132 several other published, observed and modeled studies. Section 3 also relates the SC-like
133 responses from analyses of the HALOE temperature time series [*Remsberg and Deaver,*
134 2005; *Remsberg,* 2007; *Remsberg*, 2008] and reviews how it compares with results from
135 zonal-mean models and observations. In general, there is good agreement with the model
136 predictions of the SC responses in ozone and T(p) of *Brasseur* [1993], *Marsh et al.*
137 [2007], and *Austin et al.* [2008] versus those found in the HALOE data, except in the
138 tropical upper stratosphere. Linear trends from the ozone analyses are presented in
139 Section 4, along with similar findings for the temperature from the more restricted
140 pressure-altitude range of 2 to 0.7 hPa. Section 4 also comments on a tropical to
141 subtropical anomaly in the SC-like responses of the HALOE ozone in the lower
142 stratosphere, at least as compared to the modeled responses of ozone to just the 11-yr uv-
143 flux forcing. Summary findings are in Section 5.
144
145
146

2. Approach

a. Data characteristics

HALOE is a solar occultation instrument that operated successfully on the Upper Atmosphere Research Satellite (UARS) from October 1991 through late November 2005. A description of the HALOE experiment is given in *Russell et al.* [1993], and a first characterization of its ozone profiles is provided in *Brühl et al.* [1996]. An update of the quality of the current operational ozone dataset is given in *Randall et al.* [2003] for the so-called Version 19 (or V19) Level 2 profiles that are used for the present study. The HALOE Project Team monitored the performance of the HALOE instrument over its mission lifetime, and they found no long-term degradation of its measurement characteristics that would impact the determination of a SC or long-term trend in ozone [*Gordley et al.,* 2006; *Hervig et al.,* 2007].

The HALOE ozone profiles were obtained with excellent signal-to-noise (S/N) and with no *a priori* constraints for their retrievals. They have a vertical resolution of about 2.3 km and are registered in pressure-altitude, in particular as derived from a retrieval of its own temperature profiles from about 4 hPa (near 38 km) to 0.004 hPa (near 85 km). The vertical resolution and the measurement and retrieval sensitivity of the HALOE ozone ought to be providing an accurate SC response profile, as compared with that of the more standard SBUV sounding technique, for example.

The T(p) profile information in the HALOE dataset below about the 4-hPa level was obtained from the daily 12Z operational analyses provided to the UARS Project by the

169 NOAA/Climate Prediction Center (CPC) and has relatively low vertical resolution. The
170 HALOE T(p) information above that level has a vertical resolution of 3-4 km and is
171 representative of the local times of the occultation measurements, both of which also
172 provide advantages when compared with the CPC T(p) data [*Remsberg,* 2007; *Remsberg*,
173 2008]. Thus, the HALOE ozone and T(p) datasets are compatible above the 4-hPa level
174 for obtaining SC-like responses from the upper stratosphere to the lower mesosphere and
175 for relating them to each other.
176
177 The HALOE measurements are for sunrise (SR) and sunset (SS), and there are significant
178 variations in ozone at those two times in the low to middle mesosphere due to rapidly-
179 changing, photochemical effects. First-order, diurnal corrections are included in the
180 forward model for HALOE V19 ozone above about 37 km to account for those changes
181 along the limb tangent paths for the retrieved profiles. *Natarajan et al.* [2005] re-
182 evaluated the adequacy of those corrections and developed further modifications that
183 ought to be applied to updated HALOE algorithms for the retrieval of its mesospheric
184 ozone, especially for SR conditions and above about 61 km (or about 0.2 hPa). In
185 addition, *Marsh et al.* [2003] showed that seasonal cycles for upper mesospheric ozone
186 are small at SR, but not at SS, and that it is not a good idea to combine their SR and SS
187 data for the mid mesosphere when searching for its SC response. For these reasons the
188 analyses for a SC response in this study are restricted to HALOE V19 profile segments
189 below the 0.7-hPa level (or about 53 km).
190

191 Figure 1 shows the measurement pattern of the tangent point locations from HALOE for
192 each day of 2001. One can see that the measurements were less frequent poleward of
193 about 50 degrees latitude and are missing at 40 and 50 degrees during summer. Prior to
194 1996, the summertime and mid latitude gaps are not as large because of the greater power
195 availability for instrument operations during the early years of the UARS mission. The
196 intervals for adjacent samples within a latitude zone from solar occultation measurements
197 vary from a few days to more than a month. Although rather infrequent and variable,
198 such sampling intervals are still adequate for resolving the seasonal and longer-term
199 variations from the total data record and with sufficient accuracy.
200
201 *b. Analysis procedure*
202 Some initial studies of the seasonal and longer-period variations in HALOE ozone were
203 conducted for the lower stratosphere by *Remsberg et al.* [2001] using multiple linear
204 regression (MLR) techniques, and they found that annual and quasi-biennial (QBO) terms
205 accounted for almost all of its variations. In the current study MLR was applied to
206 HALOE time series of averages of the ozone points for a given pressure layer and for 20-
207 degree wide latitude bins centered every 10 degrees from 45N to 45S. Latitude bins of
208 this width provide a high probability of having enough samples to adequately represent
209 the zonal mean. The MLR technique also accounts for the fact that the data points from
210 occultation measurements are inherently non-orthogonal. The HALOE Level 2 profiles
211 are tabulated with a spacing of 300 m. However, the precision of the data points for an
212 ozone time series was improved by linearly integrating the individual ozone profiles in
213 log pressure over "half-Umkehr layers" (about 2.5 km thick or very near to the vertical

214 resolution of the retrieved profiles). The resulting ozone amounts for those layers are
215 given in terms of Dobson Units (DU). Table 1 defines the half-Umkehr layers for this
216 study. The total pressure-altitude range is 63.3 hPa to 0.70 hPa or a range of 13 half-
217 Umkehr layers labeled from 4L to 10L, respectively.
218
219 Other researchers have reported on how the SC ozone response in the lower stratosphere
220 is confounded with and possibly dominated by decadal-scale dynamical effects [e.g.,
221 *Dunkerton and Baldwin,* 1992; *Salby et al.,* 1997]. Thus, the current study is focused on
222 the middle and upper stratosphere, where the dynamical effects are weaker and hopefully
223 more easily resolved. In most other respects the analysis approaches in *Remsberg et al.*
224 [2001] and especially in *Remsberg* [2007; 2008] were followed. Annual (AO) and semi-
225 annual (SAO) cycles were fit to the time series, and the time series residuals were
226 analyzed for their remaining interannual structure. Weak quasi-biennial or QBO-like (28
227 mo.) and sub-biennial or IA (21 mo.) terms were also found consistently in the upper
228 stratosphere. The QBO periods became more variable in the middle and lower
229 stratosphere (25 to 31 months), in accord with the power spectral analysis results of
230 HALOE ozone by *Witte et al.* [2008]. The corresponding subbiennial periods changed,
231 as well. An overall objective was to account for any significant, periodic structure in the
232 time series before analyzing for the underlying SC-like and trend terms.
233
234 The average separation in time for the points in the HALOE time series is about 25 days.
235 Even so, because zonal-average ozone values at time n have considerable memory of the
236 atmospheric state at time n-1, the time series have autoregressive characteristics. The

appropriate MLR result for that situation is obtained by a two-step process (see Appendix A of *Tiao et al.* [1990]). Initially, a model of the form,

$$O3(n) = a + bX + e \sin(Z) + f \cos(Z) + \ldots + N(n), \qquad (1)$$

was used, where O3(n) is the sum of the components of ozone at the n^{th} point in the time series. The model has a constant term 'a' and a linear term in $X = (t_n - t_1) / T$, where t_n is the time of the n^{th} observation point, t_1 is the first point in the time series, T is the total length of the time series, and b is the coefficient of the linear term. The model has seasonal and longer-period terms that are represented by Fourier components in Z, where $Z = 2\pi t_n / P$, and P is the period of a given cycle. Periodic terms that were considered are AO, SAO, QBO-like, sub-biennial (or IA), and an 11-yr (4017-dy) term. Note that the seasonal terms were almost always found to have a probability of at least 99% of being present. The QBO, IA, 11-yr, and linear terms were allowed to have lower probabilities, in order to accommodate their existence in the time series across all latitudes and pressure-altitudes. Finally, the term N(n) is the autoregressive (AR) noise residual that is given by

$$N(n) = \varphi N(n-1) + E(n), \qquad (2)$$

for a first order (or AR1) process. The factor φ is the autocorrelation of the noise residual and E(n) is the white noise component. Thus, the MLR method consists of a fit for all the terms of Eq. (1) and the generation of its model residuals N(n). The autocorrelation

coefficient φ for this model is found from the residuals. The model terms of Eq. (1) are then transformed to those of Eq. (3),

$$O3(n) - \varphi\, O3(n-1) = a[1-\varphi] + b[X(n) - \varphi\, X(n-1)] + \quad (3)$$
$$e[\sin(Z(n)) - \varphi \sin(Z(n-1)] + f[\cos(Z(n)) - \varphi \cos(Z(n-1))] + \ldots + E(n),$$

and the data time series is refit to get new coefficients. Initially, φ was set to zero for the MLR analyses using the relevant terms of Equation (1), φ was calculated from the model residuals, and then final coefficients for the terms were obtained with Equation (3). Because MLR provides for a combined fitting of all the model terms, the absolute ozone uncertainties are nearly the same for each term of the model. Percentage deviations and the probabilities of their respective terms depend on their amplitude.

Figure 2 is an example of a HALOE data time series (Layer 8U centered at about 42 km and at the latitude of 25N), where the SR and SS data have been fit with a regression model (the solid oscillatory curve) that contains the seasonal, AO and SAO terms, a QBO-like (853-dy) term, a subbiennial (640-dy) term, and an 11-yr term. The horizontal straight line is the constant term from the model, and all terms are highly significant. An 11-yr term was fit to the time series rather than regressing against a proxy term for the uv-flux, to determine whether there might be other decadal-scale terms that were affecting the ozone. The 11-yr response in Figure 2 is essentially in-phase with the time series of the solar flux for SC 22 and 23 (see following subsection, too). In other words, there is a maximum in the ozone in this case that is very near to the time of a maximum

283 in the solar flux (i.e, 0.9 yr from January 1991 and 2002), as expected from increases for
284 the uv-photodissociation of molecular oxygen [*Brasseur and Solomon,* 1984]. One can
285 also see that the maxima for the annual cycles do not exceed the horizontal line in 1996
286 and 1998, or near solar minimum; its 11-yr, maximum minus minimum response is 2.7%.
287 For this layer the amplitudes of the seasonal and interannual terms are small and of the
288 order of the amplitude of the estimated 11-yr or SC-like term. At this point it is noted
289 that the zonal mean distribution of ozone can have significant meridional variations at
290 mid and higher latitudes of the middle and upper stratosphere, yet Eq. (3) does not
291 contain a term to account for variance with latitude. Such variations are embedded
292 mainly in the coefficients of the seasonal terms. Since the latitude bins are relatively
293 narrow (20 degrees wide) compared with the meridional gradients in the zonal-average
294 ozone, the data time series provide good estimates of the true seasonal coefficients for
295 zonal-mean ozone. The aperiodic ENSO or volcanic forcings were not modeled; their
296 effects may be important for ozone in the lower stratosphere (see later).
297
298 The model fit in Figure 2 does not include a linear term, although that term is included
299 for the MLR results of Sections 3 and 4. Figure 3 is a plot of the residuals for the ozone
300 model of Figure 2. It shows that there is no remaining apparent periodic structure, which
301 is an important acceptance test for the set of terms of the final MLR model. There are
302 also no significant, non-random autocorrelations in the residuals for this final model (not
303 shown, but see *Remsberg et al.* [2001] for a diagnostic plot of this statistical test). The
304 solid horizontal line is the linear fit to the residuals; and in this case it is not significantly
305 different from zero. A polynomial trend term may account for a chemical response of

306 ozone to the long term changes in total reactive chlorine [e.g., *Randel and Wu,* 2007;
307 *Yang et al.,* 2006], but it was not included in the MLR models because reactive chlorine
308 is not the dominant loss mechanism for ozone throughout the stratosphere. Furthermore,
309 the time series of the residuals in Figure 3 does not indicate the presence of such an
310 underlying, polynomial trend term due to that chemical loss. However, since total
311 reactive chlorine reached its peak value in the upper stratosphere in the late 1990s [*WMO,*
312 2007], any enhanced chemical loss at that time would tend to reinforce the minimum
313 response of ozone to the SC forcing. Thus, the 2.7% max minus min, SC-like response of
314 the MLR model fit in Figure 2 may overestimate the amplitude of the true SC effect on
315 ozone.
316
317 Ozone is in photochemical equilibrium in the upper stratosphere, and its seasonal
318 variations are anti-correlated with the corresponding seasonal variations for HALOE
319 T(p), as shown in Figure 4 for 25N and 2 hPa. A linear trend term is included in its
320 model, and its diagnosed value is -1.1 K/decade. The 11-yr variation in T(p) is much less
321 apparent (max minus min is 0.6 K). That percentage response (0.23%) is smaller than for
322 the ozone but in accord with at least some model predictions [*Austin et al.,* 2008]. Even
323 so, the diagnosed phase for the maximum of the 11-yr term in T(p) occurs 1.7 years prior
324 to solar max and leads the 11-yr response of ozone by 2.6 years based on its MLR model
325 in Figure 2. The adjusted, in-phase, max minus min SC response is more like 0.3 K for
326 T(p). Therefore, it may be that there are other effects contributing to the analyzed, 11-yr
327 response in T(p) for this layer and latitude (see later in Section 4).
328

329 Finally, one should note that the SR and SS samples in the HALOE time series of Figures
330 2 and 4 tend to alternate, due to the sequential crossings of the orbital sampling patterns
331 for the SR and SS measurements of Figure 1. This character for the sampling leads to
332 largely real, diurnal variations in both the ozone and temperature data in the mesosphere.
333 Its occurrence enhances the 'noisy' appearance of the HALOE time series residuals after
334 removal of the seasonal and interannual terms. In addition, those alternating SR/SS
335 residuals are negatively correlated, obscuring the otherwise positive autocorrelation of
336 the residuals at lag-1 and higher lags. A first-order, average adjustment for those small,
337 SR/SS differences was obtained for these higher altitude data; mean values of the
338 separate time series of the SR and of the SS data were determined and half the difference
339 of those two means was then applied to the respective SR and SS points. This step
340 reduces the short-term, point-to-point, fluctuations in the time series and increases the
341 significance of the AR1 term and, thus, the other small amplitude terms for the regression
342 models of Figures 2 and 4, but it has essentially no effect on the phases of the periodic
343 terms. Therefore, for each time series the adjusted SR and SS points were combined,
344 giving about 200 points in all. A clearer example of this effect for the temperature tides
345 of the mesosphere can be found in *Remsberg* [2008, their Figures 1 and 2]). On the other
346 hand, almost no systematic, SR/SS differences were found for the time series of the
347 HALOE ozone in the mid and lower stratosphere, as expected based on model
348 calculations of its weak diurnal variations.
349
350

c. Signatures of interannual terms from the MLR models

Traditional proxies for the QBO term were tried during the early development of the MLR models for this study. However, QBO cycles based on the tropical lower stratospheric winds did not provide for a highly significant fit of the interannual variations in upper stratospheric ozone, particularly for the subtropics of the NH. Similar deficiencies for those QBO-proxies were reported for time series analyses of SC effects in temperature by *Crooks and Gray* [2005]. In the present study the QBO-like terms that were fitted to the ozone residuals for the low latitudes had significant changes of phase from 50 to 10 hPa, not unlike that reported by *Pascoe et al.* [2005] for the zonal winds. Thus, a QBO wind proxy that is averaged over that pressure range may not be so representative of the true forcings of that term. Furthermore, the effect of a QBO forcing in ozone is a bit more complicated because it also depends on the zonal-mean ozone distribution and its gradients, which change in magnitude and sign for the vertical range of the subtropical stratosphere. Instead, the periods and phases of the dominant interannual terms were obtained for the present study from a Fourier analysis of the points of each of the time series.

Figure 5 shows the time series of HALOE ozone observations for 25N and Layer 6L (11.2 - 15.8 hPa). The combination of the AO and SAO terms of the MLR model provides a very good fit to the seasonal variations for this layer. Amplitudes for the interannual and SC-like terms are weaker, although it is obvious that there are significant interannual variations in the data. Those variations are fit well by a combination of a 26-month QBO-like term and a 22-month subbiennial term.

373

374 The ozone of Figure 5 for 1991-92 is clearly elevated compared with that of the other
375 years, most likely a result of physical processes associated with the major volcanic
376 aerosol layer from the Mt. Pinatubo eruption of June 1991. In fact, the ozone is
377 somewhat anomalous during this period for other low to middle stratospheric layers in
378 the tropics and subtropics of both hemispheres, and Section 4 contains some discussion
379 about possible causes of the excess ozone of 1991-92. A model fit of the entire time
380 series of Figure 5 was attempted, including both a linear trend term and a periodic term of
381 11-yr period. However, the excess ozone of 1992 represents an "endpoint anomaly" for
382 the analysis. It leads to a rather large, decreasing trend and affects the nature of the
383 associated 11-yr term. Instead, for those layers that showed anomalies in this early
384 period, it was found that much more reasonable results were obtained for those two terms
385 by starting the MLR model in early September 1992 or in January 1993. That
386 modification was applied to the analyses of the layers 6U through 4L. The solid
387 oscillating curve in Figure 5 is the MLR model fit to the data using all terms, but
388 beginning in September 1992. Note also that the solid curve actually begins several
389 points later because of the need to allow for the autoregressive nature of the time series.
390

391 The 11-yr term of the model fit in Figure 5 has a "max minus min" value of 2.7%, but the
392 phase of its maximum occurs 1.0 year prior to January 1991 (or 2002). A decreasing
393 trend of 5.1%/decade was also realized from the analysis. The results for the 11-yr terms
394 from each of the 130 ozone time series are presented in Section 3. Results from similar
395 analyses of the HALOE T(p) are given there, as well, but only for the pressure layers of

396 0.7 to 2.0 hPa. Findings for the linear trend terms are presented and discussed in Section
397 4. The rest of this subsection considers the QBO-like terms and their interactions with
398 the seasonal terms.
399
400 A typical example of the zonal mean ozone distribution is shown in Figure 6 from a
401 sequence of HALOE SS observations that eventually covered most latitudes during the
402 period of February 26 to April 5, 1995. The QBO cycle has its largest effect on the zonal
403 mean ozone at the tropical latitudes and at those pressure altitudes where the vertical
404 ozone gradient is large. In fact, one can check on the realism of the current QBO signal
405 in ozone by examining its amplitudes from the analyses of the 130 separate time series, as
406 shown in Figure 7. QBO amplitudes are nearly hemispherically-symmetric throughout
407 the stratosphere. The largest amplitudes (in %) occur in the tropical stratosphere near 7
408 hPa and 30 to 40 hPa. Photochemistry controls the distribution of ozone above about the
409 5-hPa level and thus dampens the effect of the QBO on the vertical ozone gradient of the
410 upper stratosphere. Its amplitudes are also relatively weak at about 20 hPa for the
411 latitudes of 15 to 45 degrees of both hemispheres, which is where the meridional
412 gradients of ozone are weak, as well (c.f., Figures 6 and 7).
413
414 *Dunkerton* [2001] explained that a subbiennial term occurs in ozone due to the difference
415 interaction of the annual and QBO cycles. Figure 8 is a plot of the amplitudes of the
416 subbiennial terms. Again there is good continuity for the features of their distribution,
417 and their amplitudes decrease with altitude in the region of transition from dynamical to
418 photochemical control. Maximum amplitudes occur in the subtropics of the middle

419 stratosphere, where the combined effects due to the annual cycle and the QBO are largest
420 for ozone. In the tropics near 30 hPa and 7 hPa the subbiennial amplitudes are weaker
421 than that for the QBO forcing alone because the annual cycle is weak at low latitudes.
422 The subbiennial amplitudes are somewhat larger in the northern than the southern
423 hemisphere subtropics at about 10 hPa. The annual cycle amplitude is also larger for the
424 northern hemisphere in this region, presumably an indication of the zonal mean effects of
425 the more vigorous and sustained net transport during winter and springtime for the
426 northern hemisphere. The region of maximum values near 50 hPa and 30 degrees of
427 latitude is also where the annual cycle in ozone is relatively large.
428

3. Solar Cycle Responses in HALOE Data

a. Ozone

Initially, the time series of F10.7 cm solar radio flux data was employed as a proxy for the SC term, but its fit to the HALOE ozone was not significant at the 90% confidence level. That proxy term exhibited shorter period structure that was not present in the ozone time series of HALOE even after applying a smoothing to the daily values of the proxy with an 81-dy running mean to avoid the effects of the 27-dy solar rotation cycle in the daily fluxes. As mentioned earlier, there may also have been a confounding of the effects of the solar uv-flux with those from reactive chlorine during 1991-2005, at least in the upper stratosphere. Therefore, it was decided that it would to be instructive to fit an 11-yr periodic term to the time series but to allow its phase to be determined simply from its best fit to the data.

Figure 9 shows the max minus min ozone values (in percent) for its 11-yr terms over the domain of latitude and pressure-altitude. Maximum responses of order 2 to 3% were found in the upper stratosphere at subtropical to middle latitudes, and they are somewhat asymmetric between the two hemispheres. The dark shading shows where the 11-yr terms have a confidence interval (CI) of greater than 90% for their partial rank order correlations [*Remsberg et al.,* 2001], and the lighter shading indicates where they have a CI value between 70 and 90%. Max minus min values of up to 2% extend through the tropics near 3 hPa, and they remain significant at the 90% level. This finding indicates that the sampling from HALOE was adequate for representing the zonal average ozone in the tropics. In the lower stratosphere the largest percentage responses occur in the

451 subtropics of the southern hemisphere and in the tropical latitudes (although larger than
452 expected at 50 hPa). Smaller and much less significant responses occur in the tropics
453 near 1 hPa (0.5%) and from 7 to 30 hPa (1%), at low to middle latitudes of the southern
454 hemisphere near 7 hPa (1 to 1.5%), and at middle latitudes of the northern hemisphere at
455 40 hPa (1%). However, it is stressed that the estimates of significance assume that all the
456 relevant structure in the time series has been accounted for.
457
458 To see how well the diagnosed, 11-yr terms are related to the solar cycle flux, their
459 phases are given in Figure 10 in units of years from January, 1991. Due to the fact that
460 the maximum for SC 22 was broad and nearly flat over 2 years, it was assumed that the
461 11-yr signal in ozone was in-phase if it was within ±1 yr of solar uv-flux maximum (the
462 regions delineated by shading in Figure 10). SC 22 had its final peak in early 1992
463 followed by a sharp decline, and it has been argued by some that phase maximum for the
464 uv-flux occurred at that time rather than a year earlier in January 1991. But in order to be
465 consistent with the estimates of the phase of the SC maximum for T(p) of *Remsberg*
466 [2007; 2008], that January 1991 time of reference was kept for the ozone results, too.
467 Generally, the 11-yr terms for ozone are in-phase with that of the uv-flux, with the
468 exception of the upper stratosphere at tropical latitudes and near 30 hPa from the tropics
469 to northern hemisphere middle latitudes. It is presumed that the lower stratosphere
470 anomaly is indicative of an interannual, dynamical forcing mechanism that is dominating
471 the effects of the uv-forcing. In fact, *Marsh and Garcia* [2007] reported ozone at 52 hPa
472 that was anti-correlated with a lagged ENSO index; they found that this dynamical
473 forcing tended to reduce the response of ozone to a solar forcing in the lower stratosphere

474 during 1991 to 2005. Still, the results from Figure 10 indicate that the presumed ENSO
475 forcing does not seem to be affecting southern hemisphere ozone in the same way.
476
477 Figure 10 is showing that the 11-yr term has a maximum that lags that of the uv-flux by
478 several years in the tropical stratosphere from 4 to 1 hPa. This anomaly may be an
479 indication of an enhanced chemical loss of ozone due to reactive chlorine, sometime after
480 solar minimum. It is noted that such losses for annual-averaged ozone ought to be most
481 clearly evident in the upper tropical stratosphere because that is where the effects of the
482 chlorine would began to compete with those of the uv-flux [*Brasseur and Solomon*,
483 1984]. In support of this idea, it is noted that the largest values of total chlorine, as
484 inferred from the HALOE measurements, occurred from 1997 to 2002 (see Figure 1-12
485 of *WMO* [2007]). In this instance the inclusion of a simple linear, rather than a
486 polynomial, trend term in the MLR models may not adequately represent the changing
487 effects of the chlorine. Indeed, if this process is contributing to the out-of-phase, 11-yr
488 ozone response, it would be unique to the time span of the HALOE observations; that is,
489 total chlorine reached its maximum values in the upper stratosphere in the middle of its
490 14-yr period.
491
492 *b. Temperature*
493 A test of the fidelity of the ozone results is an assessment of the analogous 11-yr response
494 in temperature from HALOE, even though model simulations indicate that the percentage
495 change for T(p) ought to be much smaller than that for ozone (e.g., *Smith and Matthes*
496 [2008]). *Remsberg and Deaver* [2005] analyzed for that response using 10-degree

497 latitude bins for the upper stratosphere, as well as the mesosphere. Their MLR analysis
498 approach was essentially the same as that used here. However, they were not confident
499 of their results at and below the 3-hPa level because of concerns about the long-term
500 accuracy of the temperature time series from the NOAA/CPC to which the HALOE T(p)
501 retrievals were merged. As a result, the HALOE findings for the 11-yr and trend terms in
502 T(p) are only appropriate above the 3-hPa level for comparisons with those of ozone
503 [*Remsberg,* 2007; 2008].
504
505 The 11-yr temperature responses were obtained for 20-degree wide latitude bins in the
506 present study, in order to be compatible with the ozone results. Those responses are
507 shown in Figure 11 along with their phase deviations (in years) from January 1991 in
508 Figure 12, but only for the pressure levels of 0.7 to 2.0 hPa. The 11-yr temperature
509 maximum is in phase (within ±1 yr) with the uv-flux forcing from about 25S through
510 15N. There are transitions to somewhat out-of-phase values at 35S and at 25N, but
511 where the responses in Figure 11 are weaker and not very significant.
512
513 The HALOE 11-yr response is smaller than reported from several analyses of the long-
514 term temperature data sets from the operational satellites [*Hood,* 2004]. On the other
515 hand, the magnitude and variation with latitude and altitude for the HALOE terms at 2
516 and 1 hPa agree very well with the observed responses based on the recent findings of
517 *Crooks and Gray* [2005, their Fig. 2] for the period 1979-2001, as based on the ERA-40
518 reanalysis dataset.

519 The response in HALOE T(p) near the tropical stratopause is about two-thirds that found
520 from the simulations of *Brasseur* [1993, their Figure 14b] and about half that from the
521 fixed dynamical heating model of *McCormack and Hood* [1996]. However, the variation
522 with latitude of the HALOE response compares favorably with the model results of
523 *Marsh et al.* [2007] and of *Smith and Matthes* [2008], at least after a scaling of the latter
524 results to the actual max minus min values of the solar flux. The solar cycle response
525 from the AMTRAC model of *Austin et al.* [2008] most closely matches that reported
526 here.
527
528 The temperature response in the HALOE data is in-phase with the solar uv-flux near the
529 tropical stratopause. Thus, it is the HALOE ozone response that appears anomalous in
530 that region. However, the amplitude of the 11-yr term in ozone is becoming small and is
531 not significant at the Equator at 1 hPa. It is also noted that there was a peak in the uv-
532 flux in about January 1992, rather than January 1991. An allowance for that fact reduces
533 the phase discrepancy for ozone by 1 year without affecting the phase agreement of the
534 temperature response noticeably.
535
536 *c. Solar cycle (or SC-like) responses of HALOE ozone and temperature*
537 In order to obtain estimates of the actual response of atmospheric ozone and temperature
538 to a proxy for the direct forcing from the uv-flux, their sets of responses from Figures 9
539 and 11 have been adjusted by the amount that they were not exactly in-phase from
540 Figures 10 and 12. Those adjustments were made by multiplying the responses by the
541 factor, $\cos [2\pi\ p / 11]$, where p is the deviation of phase of the maximum (in years) from

January 1991. Even after applying the adjustments, there is good continuity among the ozone responses from the 130 separate time series.

The separate, 11-yr responses for ozone of Figure 9 have been averaged for the latitude bins that extend from 25S and 25N, and those profiles are shown in Figure 13. The corresponding, SC-like response profile is shown as well, but there is very little difference between the two. There is good similarity between the results in Figure 13 and the SC response profile obtained from the seasonally-averaged HALOE data points over the same latitude range in *Soukharev and Hood* [2006, their Figure 14], if one excludes their analyzed value at about 35 km. The magnitude and variation of the HALOE response profiles agree very well with the response at low latitudes from the representative, zonal-mean models of *Brasseur* [1993, his Figures 9a and Figure 14a] and of *Huang and Brasseur* [1993, their Figure 8a]. They also agree qualitatively with the results of *Austin et al.* [2007] and of several other models, as shown in *Soukharev and Hood* [2006, their Figure 14]. In addition, there is no discrepancy for this HALOE ozone response across most of the stratosphere versus the responses from the chemistry/climate models, AMTRAC and WACCM, in *Austin et al.* [2008].

Lee and Smith [2003] analyzed both the SAGE II and SBUV data for a solar cycle response. Their results from SAGE II are similar to the zonal mean contour values of Figure 9, at least for the upper stratosphere at most latitudes; their results from SBUV do not agree as well though, especially in the tropics (see also the analyzed results from SAGE and SBUV in *Soukharev and Hood* [2006]). *Lee and Smith* [2003] conducted

565 model studies of the SC response, but modified to account for the relative phases of the
566 QBO over specific decades. The interaction with the QBO in their model leads to larger
567 positive responses in the subtropical upper stratosphere of both hemispheres, but their
568 results are also sensitive to the QBO indexes that they employed. However, it is noted
569 that for the present HALOE analyses the interactions with the QBO and its associated
570 subbiennial term have been accounted for to first order based on the structure of those
571 terms in the HALOE time series. *Austin et al.* [2007] were able to simulate the minimum
572 ozone response at about 20 to 30 hPa, but not the analyzed, sharply increasing response at
573 about 50 hPa in Figure 13. The model simulations reported in *Marsh et al.* [2007, their
574 Figure 8] indicated a positive ozone response near 50 hPa at low latitudes for the period
575 of 1979 to 2003, but not for the longer period of 1950 to 2003. It is presumed that the
576 large response diagnosed from the HALOE data is not strictly related to the solar cycle.
577
578 The SC-like, max minus min responses for ozone (in percent) and for temperature (in K)
579 are summarized in Table 2 for the region of the stratopause and for three distinct latitude
580 zones, 45S to 35S, 15S to 5N, and 25N to 45N. For the tropical latitude zone the adjusted
581 ozone response is small and not significant, while the associated temperature response is
582 1.0 K and highly significant. For the middle latitude zones the ozone response varies
583 between 1.9 and 2.8% and is highly significant, while the temperature response decreases
584 to near zero.
585

4. Trends in HALOE ozone

Figure 14 shows the linear trends (in %/decade) obtained from the MLR analyses of the HALOE ozone. Darker shading is where those terms have a CI of greater than 90%; lighter shading denotes a CI between 70 and 90%. The trends are near zero in the upper stratosphere across most of the latitude domain and for this 14-yr time span, when the total chlorine levels had leveled off and started to decline slowly [*WMO*, 2007]. The trends are decreasing by 4 to 6 %/decade across most latitudes of the middle stratosphere, and they are significant. There are net increases in the ozone of the lower stratosphere in the subtropics of both hemispheres, but slight decreases in the tropics. Those trends are not significant, however. Overall, there is very good continuity in the patterns of the trends for the latitude and pressure-altitude domain of Figure 14.

The trends shown in Figure 14 appear to be somewhat weaker than those reported from HALOE, SAGE II, and lidar in *WMO* [2007]. However, those analyses were for data time series on constant altitude surfaces, and it is noted that the effects of a long-term cooling of the atmosphere will lead to a lowering in altitude of a pressure surface and its ozone [*Rosenfield et al.*, 2005]. For example, the temperature trends reported by *Remsberg* [2007; 2008] for 25S to 25N are of order -0.8 to -1.2 K/decade for the pressure surfaces of 0.7 to 2.0 hPa, respectively, or for those levels where it is possible to conduct reliable analyses for a temperature trend from retrievals of the HALOE measurements themselves. Thus, a negative ozone trend at an altitude level will appear as a weaker trend at a corresponding pressure level.

608 There may also be slight biases in the analyzed trends from the HALOE zonal-averaged
609 ozone versus pressure profiles at all latitudes for the layers 7L to 4U. This prospect is
610 because the HALOE T(p) profiles for those layers were based on the data from the
611 NOAA operational temperature sounders that were not corrected for the trends in the
612 atmospheric CO_2, as they affect the vertical weighting functions of their several
613 measurement channels [*Shine et al.*, 2008]. However, any such effects should not alter
614 the trends with latitude in Figure 14 for a given pressure layer.
615
616 A number of investigators have wondered to what extent the eruption of Mt. Pinatubo
617 may have affected the SC-like and trend terms for ozone [e.g., *Lee and Smith,* 2003; *Al-*
618 *Saadi et al.,* 2001]. Furthermore, *Crooks and Gray* [2005] point out that there were
619 interactions between the QBO and ENSO that were altering the zonal winds of the
620 subtropical middle stratosphere both prior to and just following the eruption of Mt.
621 Pinatubo. Recall from Figure 5 that there was an excess of ozone in layer 6L at 25N
622 during late 1991 to mid 1992. That excess may be related to atmospheric effects due to
623 the presence of the Pinatubo aerosol layer [*Mickley et al.,* 1997]. For example, the
624 radiative heating at the top boundary of the aerosol layer (near 20 hPa) can lead to an
625 enhanced, net ascent at the low latitudes. As a result, air having a relatively low mixing
626 ratio of NOy would have been transported upward from the lower stratosphere, and the
627 associated chemical loss of ozone due to the reactive, NOx component of the NOy would
628 have been diminished at that time. There are similar excess ozone anomalies in the layers
629 6U through 5U (or about 10 to 20 hPa), at least for the latitude bins of 25S through 25N,
630 and they lead to excessively negative linear trends when the time series analyses are

631 started at October 1991 rather than September 1992 or January 1993. In addition, there
632 are greater uncertainties for the ozone signals that were attenuated by the aerosols of the
633 lower layers of the low latitudes during this early period, so the analyses of their time
634 series were begun at those later times, too. A further diagnosis of the true cause of the
635 enhanced HALOE ozone in 1991-92 at 10 to 20 hPa is outside the scope of this study, but
636 that ozone excess represents an "end point anomaly" for the determination of the trend
637 terms (and for the coefficients of the associated 11-yr terms to a lesser extent). By
638 delaying the start date of the time series analyses by at least one year after the eruption
639 but only for layers 6U to 4U of the lower latitudes, the effects from the volcanic aerosol
640 layer have been reduced for the results of this present study.
641
642 The narrow pressure-altitude zone of rather large negative trends at 10 to 20 hPa in
643 Figure 14 may have contributions from structures in those time series that were not
644 accounted for. To understand that possibility, it is useful to refer to the representative
645 zonal mean cross section of the HALOE ozone mixing ratio in Figure 6. In the low to
646 middle stratosphere the ozone mixing ratio should be very nearly conserved during
647 transport. Any change for its net transport at those altitudes ought to be most noticeable
648 where the meridional gradients of the ozone mixing ratio are greatest, or in the subtropics
649 near 10 hPa. The latitudes of 15 to 25 degrees are where the diagnosed 11-yr ozone
650 responses of Figure 9 are larger. That region is also where the amplitudes of both the
651 QBO and subbiennial terms are pronounced (see Figures 7 and 8). It may be that the
652 larger negative trends and the enhanced SC-like responses in that region have a
653 contribution from a decadal-scale, dynamical forcing. On the other hand, because the

654 meridional gradients for the ozone mixing ratio are nearly flat at about 20 hPa, the
655 presence of a similar dynamical forcing would be much less apparent in the ozone at that
656 level. There are also larger negative trends that are marginally significant at 45S and 45N
657 and from 30 to 50 hPa. Perhaps those trends are indicating an extension of so-called
658 "polar ozone hole" effects to lower latitudes during this 14-yr period. If that is the case,
659 it is noted that the effects of the QBO term for the lower stratospheric ozone distributions
660 have already been accounted for as part of the present MLR analyses.
661

5. Summary and Conclusions

This study has been based on ozone and temperature data from a single, well-characterized instrument, HALOE, and for slightly more than one complete solar cycle. An exploratory search for a solar cycle response was performed, but only for those latitudes where HALOE provided good seasonal sampling. This consideration is important for the accurate accounting of the generally, larger-amplitude seasonal terms in the time series. The HALOE ozone profiles have good S/N and a relatively high vertical resolution, both of which are important for resolving the vertical response of ozone to the relatively, small amplitude of the 11-yr, max minus min, uv-flux forcing. Analyses of temperature time series were restricted to the upper stratosphere and lower mesosphere, 2.0 to 0.7 hPa.

The analyzed QBO terms for ozone have their largest amplitudes at the low latitudes and in the lower stratosphere, and their amplitudes are nearly symmetric with latitude across the two hemispheres. On the other hand, there is some asymmetry for the amplitudes of the sub-biennial terms, in accord with the small differences for its associated annual cycles in the two hemispheres. There may also be interactions between the QBO and sub-biennial terms, but their longer-period terms were not included in the analyses.

A simple, 11-yr periodic term was fit to the ozone residuals, and its phase was noted. Where the amplitude of that term was significant, its phase fit with that of the SC flux proxies, or at least within about one year of January 1991 (or 2002)—the approximate midpoint for the flux maximum of SC 22 (or SC 23). Because the effects of trend terms

684 can be confounded with those of the 11-yr terms, linear trend terms were included in the
685 MLR analysis model. Generally, there is very good continuity for the analyzed trends
686 with latitude and pressure-altitude, and their signs and magnitudes are reasonable for the
687 time period of 1991-2005 from the HALOE measurements. However, it is noted that
688 there may still be decadal-scale processes that were important, but not accounted for—
689 particularly in the upper stratosphere of the tropics and in the lower stratosphere across
690 all latitudes.
691
692 There is a significant SC-like, max minus min response of order 2 to 3% in the HALOE
693 ozone from about 2 to 5 hPa and for the latitudes of 45S to 45N. Weaker and much less
694 significant responses occur in the tropics near 1 hPa and from 7 to 30 hPa. There is a
695 significant max minus min, SC-like response of order 1 K in the HALOE temperatures
696 between 15S and 15N and from 2 to 0.7 hPa. The temperature response at mid latitudes
697 is about half that value and much less significant. Several chemistry/climate models are
698 yielding response profiles for both ozone and temperature that are very similar to those
699 analyzed here [*Austin et al.,* 2008].
700
701 As noted above, linear trends were diagnosed along with the other terms of the MLR
702 analyses of the HALOE ozone, and they were near zero throughout the upper
703 stratosphere. Negative trends of order 4 to 6%/decade were found at 10 to 20 hPa across
704 the low to middle latitudes of both hemispheres. Weak, positive trends were found in the
705 lower stratosphere for the subtropics of both hemispheres. Conversely, there were weak,

706 negative trends from 30 to 50 hPa in the tropics and poleward of about 25 degrees
707 latitude of both hemispheres.
708
709 It is concluded that there is no real discrepancy between the SC-like response profiles
710 from some current models and from the stratospheric ozone from the HALOE
711 observations, at least where its SC-like terms are significant. The MLR analysis
712 approach used herein has made it possible to separate that response from those of the
713 expected interannual forcings and to first order from the confounding effects of any long-
714 term trends. The precision, calibration, vertical resolution, spatial sampling , and
715 retrieval approach of the HALOE solar occultation experiment along with the MLR
716 analysis techniques used herein appear to be quite adequate for future determinations of
717 the middle atmosphere responses of both ozone and temperature to the uv-flux forcing of
718 the 11-yr solar cycle.
719
720

Acknowledgments. The author embarked on this analysis as a result of his invitation to participate in a Workshop hosted by Dr. Kunihiko Kodera at the 2004 Fall AGU Meeting. The author appreciates discussions about this work that he has had with two colleagues—Murali Natarajan, concerning comparisons of the findings with published results from model studies, and Gretchen Lingenfelser concerning the MLR analyses. Special thanks go to Jim Russell, HALOE Principal Investigator, and Larry Gordley and colleagues of GATS, Inc., for producing the high quality HALOE dataset. He also appreciates the comments of the three anonymous reviewers. Support for this work was provided by the UARS Program Office at NASA Headquarters and the UARS Project Office at NASA/GSFC.

730 **References**

731 Al-Saadi, J. A., R. B. Pierce, T. D. Fairlie, M. M. Kleb, R. S. Eckman, W. L. Grose, M.
732 Natarajan, and J. R. Olson (2001), Response of middle atmosphere chemistry and
733 dynamics to volcanically elevated sulfate aerosol: three-dimensional coupled model
734 simulations, *J. Geophys. Res., 106*, 27,255-27,275.
735
736 Anderson, J., and J. M. Russell III (2004), Long-term changes of HCl and HF as
737 observed by HALOE, in *Proceedings Quadrennial Ozone Symposium*, Kos, Greece, 223-
738 224.
739
740 Austin, J., L. L. Hood, and B. E. Soukharev (2007), Solar cycle variations of
741 stratospheric ozone and temperature in simulations of a coupled chemistry-climate
742 model, *Atmos. Chem. Phys., 7,* 1693-1706.
743
744 Austin, J., et al. (2008), Coupled chemistry climate model simulations of the solar cycle
745 in ozone and temperature, *J. Geophys. Res., 113*, D11306, doi:10.1029/2007JD009391.
746
747 Brasseur, G. (1993), The response of the middle atmosphere to long-term and short-term
748 solar variability: a two-dimensional model, *J. Geophys. Res., 98*, 23,079-23,090.
749
750 Brasseur, G., and S. Solomon (1984), *Aeronomy of the Middle Atmosphere*, D. Reidel
751 Publ. Co., Dordrecht, Holland, 441 pp.
752

753 Brühl, C., et al. (1996), Halogen occultation experiment ozone channel validation, *J.*
754 *Geophys. Res., 101*, 10,217-10,240.
755
756 Callis, L. B., M. Natarajan, and J. D. Lambeth (2000), Calculated upper stratospheric
757 effects of solar uv flux and NOy variations during the 11-year solar cycle, *Geophys. Res.*
758 *Lett., 27,* 3869-3872.
759
760 Chandra, S., and R. McPeters (1994), The solar cycle variation of ozone in the
761 stratosphere inferred from Nimbus 7 and NOAA 11 satellites, *J. Geophys. Res., 99*,
762 20,665-20,671.
763
764 Crooks, S. A., and L. J. Gray (2005), Characterization of the 11-year solar signal using a
765 multiple regression analysis of the ERA-40 dataset, *J. Climate, 18*, 996-1015.
766
767 Cunnold, D. M., E.-S. Yang, M. J. Newchurch, G. C. Reinsel, J. M. Zawodny, and J. M.
768 Russell III (2004), Comment on "Enhanced upper stratospheric ozone: sign of recovery
769 or solar cycle effect?" by W. Steinbrecht et al., *J. Geophys. Res., 109*, D14305,
770 doi:10.1029/2004JD004826.
771
772 Dunkerton, T. J. (2001), Quasi-biennial and subbiennial variations of stratospheric trace
773 constituents derived from HALOE observations, *J. Atmos. Sci., 58*, 7-25.
774

775 Dunkerton, T. J., and M. P. Baldwin (1992), Modes of interannual variability in the
776 stratosphere, *Geophys. Res. Lett., 19*, 49-52.
777
778 Fleming, E. L., S. Chandra, C. H. Jackman, D. B. Considine, and A. R. Douglass (1995),
779 The middle atmospheric response to short and long term solar uv variations: an analysis
780 of observations and 2D model results, *J. Atmos. Terr. Phys., 57*, 333-365.
781
782 Garcia, R. R., S. Solomon, R. G. Roble, and D. W. Rusch (1984), A numerical response
783 of the middle atmosphere to the 11-year solar cycle, *Planet. Space Sci., 32*, 411-423.
784
785 Gordley, L. L., M. E. Hervig, R. E. Thompson, B. E. Magill, J. M. Russell, and E. E.
786 Remsberg (2006), Detector nonlinearity effects on the HALOE data (preliminary results),
787 *Eos Trans. AGU, 87(52)*, Fall Meet. Suppl., Abstract A21F-0908.
788
789 Harris, N., R. Hudson, and C. Phillips, (Eds.) (1998), Assessment of trends in the vertical
790 distribution of ozone, *SPARC Rep. #1*, 289 pp., World Meteorol. Org., Geneva.
791
792 Hervig, M., L. Gordley, M. McHugh, E. Thompson, B. Magill, and L. Deaver (2007),
793 On-orbit calibration of HALOE detector linearity, *Appl. Opt., 46*, 7811-7816.
794
795 Hood, L. (2004), Effects of solar uv variability on the stratosphere, in *Solar Variability*
796 *and its Effects on Climate*, Geophysical Monograph 141, AGU, 283-303.
797

798 Huang, T. Y. W., and G. P. Brasseur (1993), Effect of long-term solar variability in a
799 two-dimensional interactive model of the middle atmosphere, *J. Geophys. Res., 98*,
800 20,413-20,427.
801
802 Kodera, K., and Y. Kuroda (2002), Dynamical response to the solar cycle, *J. Geophys.,*
803 *Res., 107*, D24, 4749, doi:10.1029/2002JD002224.
804
805 Lee, H., and A. K. Smith (2003), Simulation of the combined effects of solar cycle,
806 quasi-biennial oscillation, and volcanic forcing on stratospheric ozone changes in recent
807 decades, *J. Geophys. Res., 108*, no. D2, 4049, doi:10.1029/2001JD001503.
808
809 Matthes, K., U. Langematz, L. L. Gray, K. Kodera, and K. Labitzke (2004), Improved
810 11-solar signal in the Freie Universitat Berlin Climate Middle Atmosphere Model (FUB-
811 CMAM), *J. Geophys. Res., 109*, D06101, doi:10.1029/2003JD004012.
812
813 Marsh, D. R., and R. R. Garcia (2007), Attribution of decadal variability in lower-
814 stratospheric tropical ozone, *Geophys. Res. Lett., 34*, L21807,
815 doi:10.1029/2007GL030935.
816
817 Marsh, D. R., R. R. Garcia, D. E. Kinnison, B. A. Boville, F. Sassi, S. C. Solomon, and
818 K. Matthes (2007), Modeling the whole atmosphere response to solar cycle changes in
819 radiative and geomagnetic forcing, *J. Geophys. Res., 112*, D23306,
820 doi:10.1029/2006JD008306.

821

822 Marsh, D., A. Smith, and E. Noble (2003), Mesospheric ozone response to changes in
823 water vapor, *J. Geophys. Res., 108*, D3, 4109, doi:10.1029/2002JD002705.
824

825 McCormack, J. P., D. E. Siskind, and L. L. Hood (2007), Solar-QBO interaction and its
826 impact on stratospheric ozone in a zonally averaged photochemical transport model of the
827 middle atmosphere, *J. Geophys. Res.,112,* D16109, doe:10.1029/2006JD008369.
828

829 McCormack, J. P., and L. L. Hood (1996), Apparent solar cycle variations of upper
830 stratospheric ozone and temperature: latitude and seasonal dependences, *J. Geophys.*
831 *Res., 101*, 20,933-20,944.
832

833 Mickley, L. J., J. P. D. Abbatt, J. E. Frederick, and J. M. Russell III (1997), Response of
834 summertime odd nitrogen and ozone at 17 mbar to Mount Pinatubo aerosol over the
835 southern midlatitudes: observations from the Halogen Occultation Experiment, *J.*
836 *Geophys. Res., 102,* no. D19, 23,537-23,582.
837

838 Natarajan, M., L. E. Deaver, E. Thompson, and B. Magill (2005), Impact of twilight
839 gradients on the retrieval of mesospheric ozone from HALOE, *J. Geophys. Res., 110,*
840 D13305, doi:1029/2004JD005719.
841

842 Nedoluha, G. E., et al. (1998), Increases in middle atmospheric water vapor as observed
843 by the ground-based Water Vapor Millimeter-wave Spectrometer and HALOE from
844 1991-1997, *J. Geophys. Res., 103*, 3531-3544.
845
846 Newchurch, M. J., E-S. Yang, D. M. Cunnold, G. C. Reinsel, J. M. Zawodny, and J. M.
847 Russell III (2003), Evidence for slowdown in stratospheric ozone loss: first stage of
848 ozone recovery, *J. Geophys. Res., 108*, no. D16, 4507, doi:10.1029/2003JD003471.
849
850 Nissen, K. M., K. Matthes, U. Langematz, and B. Mayer (2007), Towards a better
851 representation of the solar cycle in general circulation models, *Atmos. Chem. Phys., 7,*
852 5391-5400.
853
854 Pascoe, C. L., L. J. Gray, S. A. Crooks, M. N. Juckes, and M. P. Baldwin (2005), The
855 quasi-biennial oscillation: analysis using ERA-40 data, *J. Geophys. Res., 110*, D08105,
856 doi:10.1029/2004JD004941.
857
858 Randall, C. E., et al. (2003), Validation of POAM III ozone: comparisons with
859 ozonesonde and satellite data, *J. Geophys. Res., 108*, no. D12, 4367,
860 doi:10:1029/2002JD002944.
861
862 Randel, W. J., and F. Wu (2007), A stratospheric ozone profile data set for 1979-2005:
863 variability, trends, and comparisons with column ozone data, *J. Geophys. Res., 112,*
864 D06313, doi:10.1029/2006JD007339.

865

866 Randel, W. J., F. Wu, J. M. Russell III, J. M. Zawodny, and J. Nash (2000), Interannual
867 changes in stratospheric constituents and global circulation derived from satellite data, in
868 *Atmospheric Science Across the Stratopause*, Geophysical Monograph 123, AGU, 271-
869 285.

870

871 Reinsel, G. C. (2002), Trend analysis of upper stratospheric Umkehr ozone data for
872 evidence of turnaround, *Geophys. Res. Lett., 29*, no. 10, doi:10.1029/2002GL014716.

873

874 Reinsel, G. C., E. C. Weatherhead, G. C. Tiao, A. J. Miller, R. M. Nagatani, D. J.
875 Wuebbles, and L. E. Flynn (2002), On detection of turnaround and recovery in trend for
876 ozone, *J. Geophys. Res., 107*, no. D10, 4078, 10.1029/2001JD000500.

877

878 Remsberg, E. E. (2008), On the observed changes in upper stratospheric and mesospheric
879 temperatures from UARS HALOE, in Special Issue entitled 'Long-Term Changes and
880 Trends in the Atmosphere', *Annales Geophysicae*, *26*, 1287-1297.

881

882 Remsberg, E. E. (2007), A re-analysis for the seasonal and longer-period cycles and the
883 trends in middle-atmosphere temperature from Halogen Occultation Experiment, *J.*
884 *Geophys. Res., 112*, D09118, doi:10.1029/2006JD007489.

885

886 Remsberg, E. E., and L. E. Deaver (2005), Interannual, solar cycle, and trend terms in
887 middle atmospheric temperature time series from HALOE, *J. Geophys. Res., 110*,
888 D06106, doi:10.1029/2004JD004905.
889
890 Remsberg, E. E., P. P. Bhatt, and L. E. Deaver (2001), Ozone changes in the lower
891 stratosphere from the halogen occultation experiment for 1991 through 1999, *J. Geophys.*
892 *Res., 106*, 1639-1653.
893
894 Rosenfield, J. E., S. M. Frith, and R. S. Stolarski (2005), Version 8 SBUV ozone profile
895 trends compared with trends from a zonally averaged chemical model, *J. Geophys. Res.,*
896 *110*, D12302, doi:10.1029/2004JD005466.
897
898 Rozanov, E. V., M. E. Schlesinger, T. A. Egorova, B. Li, N. Andronova, and V. A.
899 Zubov (2004), Atmospheric response to the observed increase of solar UV radiation from
900 solar minimum to solar maximum simulated by the University of Illinois at Urbana-
901 Champaign climate-chemistry model, *J. Geophys. Res., 109*, D01110,
902 doi:10.1029/2003JD003796.
903
904 Russell, J. M. III, L. L. Gordley, J. H. Park, S. R. Drayson, D. H. Hesketh, R. J. Cicerone,
905 A. F. Tuck, J. E. Frederick, J. E. Harries, and P. J. Crutzen (1993), The Halogen
906 Occultation Experiment, *J. Geophys. Res., 98*, 10,777-10,797.
907

908 Salby, M., P. Callaghan, and D. Shea (1997), Interdependence of the tropical and
909 extratropical QBO: relationship to the solar cycle versus a biennial oscillation in the
910 stratosphere, *J. Geophys. Res., 102*, 29,789-29,798.
911
912 Scaife, A. A., J. Austin, N. Butchart, S. Pawson, M. Keil, J. Nash, and I. N. James (2000),
913 Seasonal and interannual variability of the stratosphere diagnosed from UKMO TOVS
914 analyses, *Quart. J. Roy. Meteorol. Soc., 126*, 2585-2604.
915
916 Shindell, D., D. Rind, N. Balachandran, J. Lean, and P. Lonergan (1999), Solar cycle
917 variability, ozone, and climate, *Science, 284*, 305-308.
918
919 Shine, K. P., J. J. Barnett, and W. J. Randel (2008), Temperature trends derived from
920 Stratospheric Sounding Unit radiances: the effect of increasing CO_2 on the weighting
921 function, *Geophys. Res. Lett., 35*, L02710, doi:10.1029/2007GL032218.
922
923 Siskind, D. E., L. Froidevaux, J. M. Russell, and J. Lean (1998), Implications of upper
924 stratospheric trace constituent changes observed by HALOE for O3 and ClO from 1992-
925 1995, *Geophys. Res. Lett., 25*, 3513-3516.
926
927 Smith, A. K., and K. Matthes (2008), Decadal-scale periodicities in the stratosphere
928 associated with the solar cycle and the QBO, *J. Geophys. Res., 113*, D05311,
929 doi:10.10292007JD009051.
930

931 Solomon, S., R. W. Portmann, R. R. Garcia, L. W. Thomason, L. R. Poole, and M. P.
932 McCormick (1996), The role of aerosol variations in anthropogenic ozone depletion at
933 northern midlatitudes, *J. Geophys. Res., 101*, 6713-6727.
934
935 Soukharev, B. E., and L. L. Hood (2006), Solar cycle variation of stratospheric ozone:
936 multiple regression analysis of long-term satellite data sets and comparisons with models,
937 *J. Geophys. Res., 111*, D20314, doi:10.1029/2006JD007107.
938
939 Steinbrecht, W., H. Claude, and P. Winkler (2004a), Enhanced upper stratospheric ozone:
940 sign of recovery or solar cycle effect?, *J. Geophys. Res., 109*, D02308,
941 doi:10.1029/2003JD004284.
942
943 Steinbrecht, W., H. Claude, and P. Winkler (2004b), Reply to comment by D. M.
944 Cunnold et al. on "Enhanced upper stratospheric ozone: sign of recovery or solar cycle
945 effect?", *J. Geophys. Res., 109*, D14306, doi:10.1029/2004JD004948.
946
947 Tian, W., M. P. Chipperfield, L. L. Gray, and J. M. Zawodny (2006), Quasi-biennial
948 oscillation and tracer distributions in a coupled chemistry-climate model, *J. Geophys.*
949 *Res., 111,* D20301, doi:10.1029/2005JD006871.
950
951 Tiao, G. C., G. C. Reinsel, D. Xu, J. H. Pedrick, X. Zhu, A. J. Miller, J. J. DeLuisi, C. L.
952 Mateer, and D. J. Wuebbles (1990), Effects of autocorrelation and temporal sampling

953 schemes on estimates of trend and spatial correlation, *J. Geophys. Res., 95*, 20,507-
954 20,517.
955
956 Wang, H. J., D. M. Cunnold, and X. Bao (1996), A critical analysis for Stratospheric
957 Aerosol and Gas Experiment ozone trends, *J. Geophys. Res., 101*, 12, 495-12,514.
958
959 Weatherhead, E. C., et al. (1998), Factors affecting the detection of trends: statistical
960 considerations and applications to environmental data, *J. Geophys. Res., 103*, 17,149-
961 17,161.
962
963 Witte, J. C., M. R. Schoeberl, A. R. Douglass, and A. M. Thompson (2008), The quasi-
964 biennial oscillation and annual variations in tropical ozone from SHADOZ and HALOE,
965 *Atmos. Chem. Phys. Discuss., 8*, 6355-6378.
966
967 World Meteorological Organization (2007), *Scientific assessment of ozone depletion:*
968 *2006,* Global Ozone Research and Monitoring Project, Rept. No. 50, 572 pp., Geneva,
969 Switzerland.
970
971 Yang, E-S., D. M. Cunnold, R. J. Salawitch, M. P. McCormick, J. M. Russell III, J. M.
972 Zawodny, S. Oltmans, and M. J. Newchurch (2006), Attribution of recovery in lower-
973 stratospheric ozone, *J. Geophys. Res., 111*, D17309, doi:10.1029/2005JD006371.

974 **Figure 1**. Tangent point locations of the HALOE SR and SS measurements for 2001.

975

976 **Figure 2**. Time series of ozone (in DU) for half-Umkehr layer 8U (near 2.4 hPa) at 25N.

977 MLR model terms are indicated at the lower left.

978

979 **Figure 3**. Time series residuals for the ozone model of Figure 2. The solid horizontal

980 line is the least squares linear regression fit to the residuals.

981

982 **Figure 4**. Time series of temperature (in K) at 2 hPa and 25N. MLR model terms are

983 indicated at the lower left. The solid horizontal line is the sum of its constant and linear

984 trend terms.

985

986 **Figure 5**. Time series of ozone for half-Umkehr layer 6L (near 13 hPa) at 25N. MLR

987 model terms are indicated at the lower left, and the fit to the data starts in September,

988 1992.

989

990 **Figure 6**. Zonal mean cross section of the HALOE ozone mixing ratio (in ppmv) for

991 sunset (SS) from February 26 to April 5, 1995. Contour interval is 1 ppmv.

992

993 **Figure 7**. Contour plot of the amplitude (in %) of the QBO term for the HALOE ozone

994 from the MLR models. Contour interval is 0.5% from 0.0 to 5.0 and 2.0% thereafter.

995 Darker shading is where the amplitudes exceed 2%.

996

Figure 8. As in Figure 7, but for the amplitudes of the sub-biennial terms.

Figure 9. Contour plot of the max minus min 11-yr response (in percent) for HALOE ozone. Contour interval is 0.5% from 0.0 to 5% and is 2% thereafter. Darker shading denotes regions where the response exceeds a CI of 90%; lighter shading has a CI of between 70 and 90%.

Figure 10. Phase variation of the 11-yr term of Figure 9 (in yrs from January 1991). Contours are: dashed—negative, solid—positive, and dotted—zero, and the interval is 1 yr. The domain within the bold contours of +1 and -1 is considered as in-phase with the SC uv-flux and that region is shaded darker.

Figure 11. Contour plot of the max minus min 11-yr response (in K) for HALOE temperature. Contour interval is 0.2 K. Darker shading denotes regions where the response exceeds a CI of 90%; lighter shading has a CI of between 70 and 90%.

Figure 12. Phase variation of the 11-yr term of Figure 11 (in years from January 1991). Contours are: dashed—negative, solid—positive, and dotted—zero, and the interval is 1 yr. The domain within the bold contours of +1 and -1 is considered as in-phase with the SC uv-flux and that region is shaded darker.

1018 **Figure 13**. Profiles of the 11-yr and the SC-like, max minus min responses (in percent)
1019 for the tropical to subtropical ozone from HALOE. The solid curve is the model result
1020 for 5N from *Brasseur* [1993].
1021
1022 **Figure 14**. Contour plot of the linear trend terms (in %/decade) from the MLR models of
1023 HALOE ozone. Contour interval is 2%; the positive and zero contours are solid, while
1024 the negative contours are dashed. Darker shading denotes regions where the trend has a
1025 CI exceeding 90%; lighter shading has a CI of between 70 and 90%.
1026

Table 1—Pressure Intervals and Half-Umkehr Layer Designations

Pressure Range in (hPa)	Half-Umkehr Layer
0.7- 1.0	10L
1.0- 1.4	9U
1.4- 2.0	9L
2.0- 2.8	8U
2.8- 4.0	8L
4.0- 5.6	7U
5.6- 7.9	7L
7.9-11.2	6U
11.2-15.8	6L
15.8-22.4	5U
22.4-31.7	5L
31.7-44.8	4U
44.8-63.3	4L

Table 2—SC-like, max minus min responses for ozone (%) and temperature (K)

	35S to 45S		15S to 5N		25N to 45N	
P(hPa)	Ozone	T(p)	Ozone	T(p)	Ozone	T(p)
0.85	1.9	0.1	0.0	0.9	2.1	0.1
1.2	2.0	0.1	-0.2	1.1	2.8	-0.1
1.7	2.7	-0.2	0.1	1.0	2.6	0.1

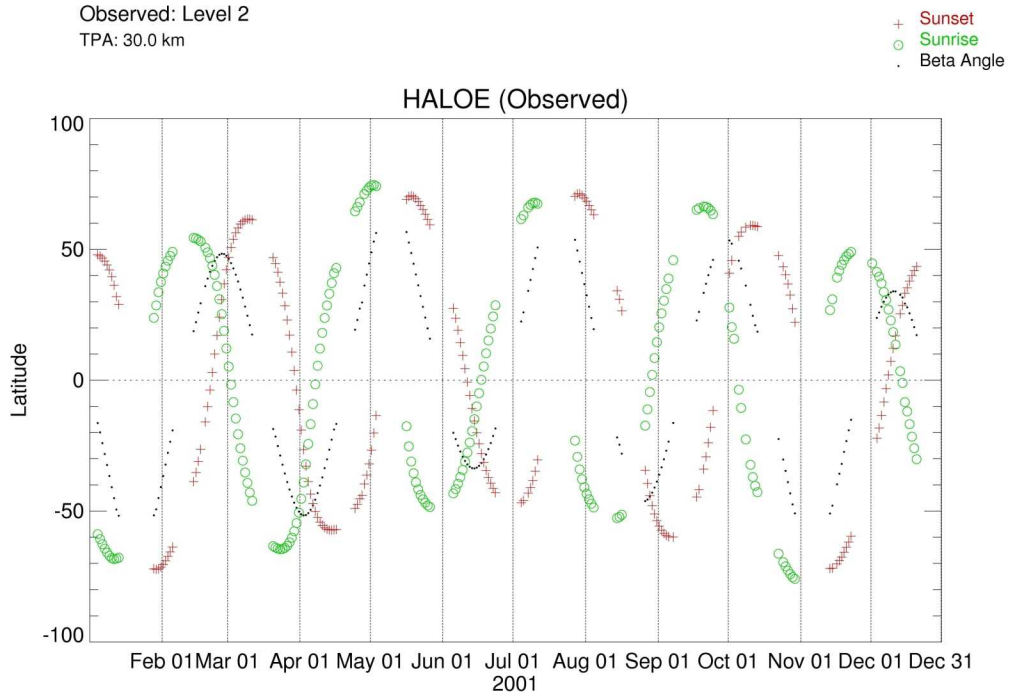

Figure 1. Tangent point locations of the HALOE SR and SS measurements for 2001.

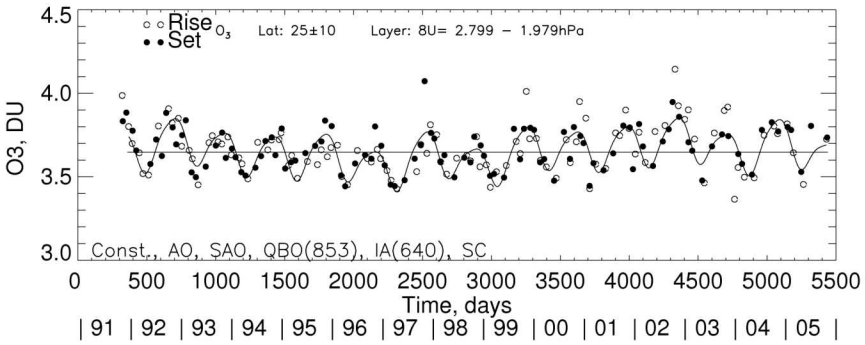

Figure 2. Time series of ozone (in DU) for half-Umkehr layer 8U (near 2.4 hPa) at 25N. MLR model terms are indicated at the lower left.

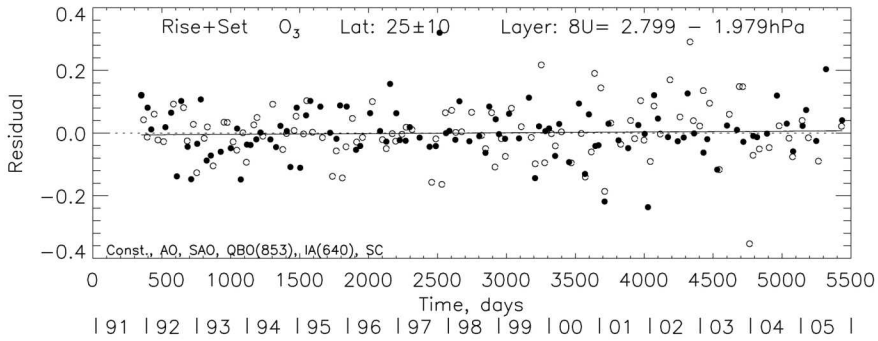

Figure 3. Time series residuals for the ozone model of Figure 2. The solid horizontal line is the least squares linear regression fit to the residuals.

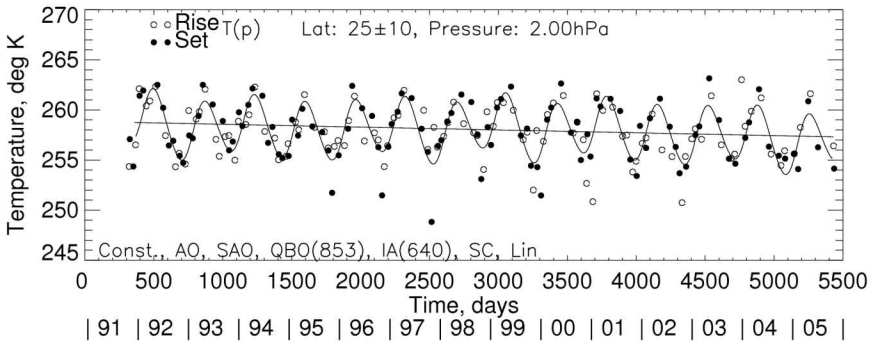

Figure 4. Time series of temperature (in K) at 2 hPa and 25N. MLR model terms are indicated at the lower left. The solid horizontal line is the sum of its constant and linear trend terms.

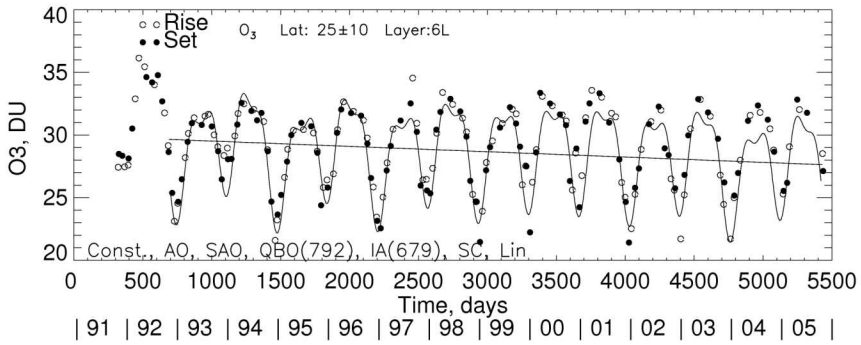

Figure 5. Time series of ozone for half-Umkehr layer 6L (near 13 hPa) at 25N. MLR model terms are indicated at the lower left, and the fit to the data starts in September, 1992.

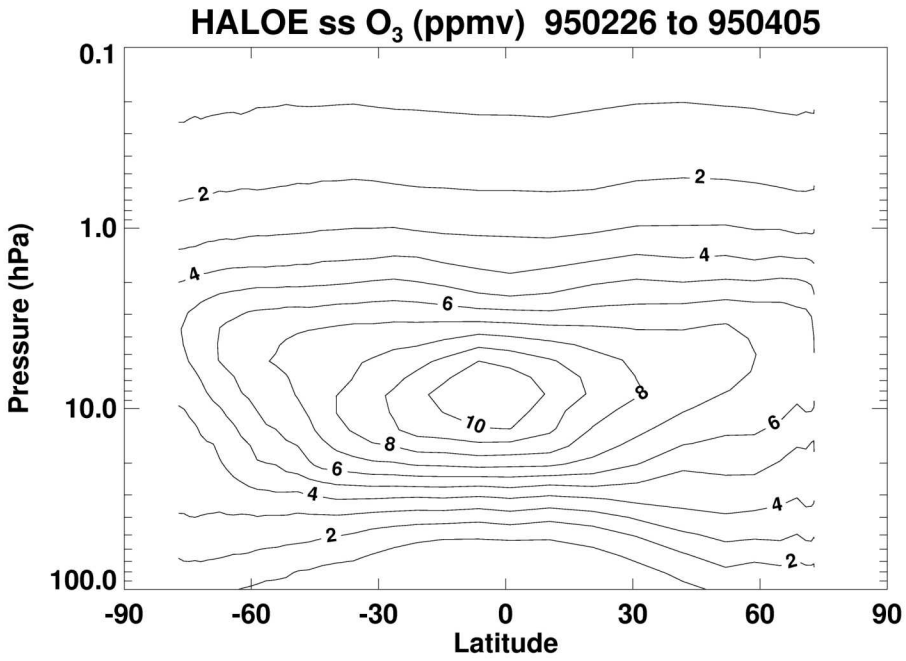

Figure 6. Zonal mean cross section of the HALOE ozone mixing ratio (in ppmv) for sunset (SS) from February 26 to April 5, 1995. Contour interval is 1 ppmv.

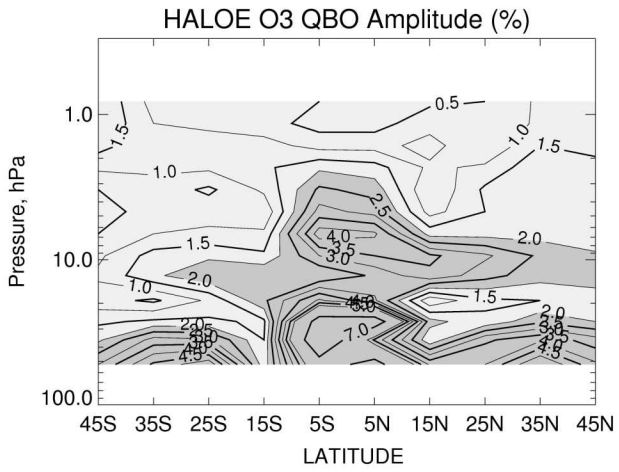

Figure 7. Contour plot of the amplitude (in %) of the QBO term for the HALOE ozone from the MLR models. Contour interval is 0.5% from 0.0 to 5.0 and 2.0% thereafter. Darker shading is where the amplitudes exceed 2%.

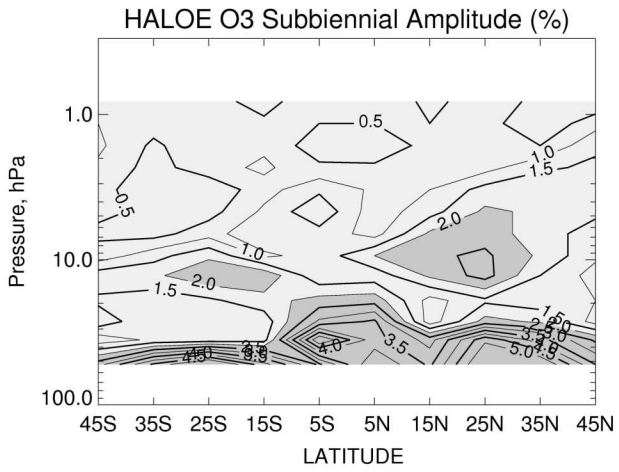

Figure 8. As in Figure 7, but for the amplitudes of the sub-biennial terms.

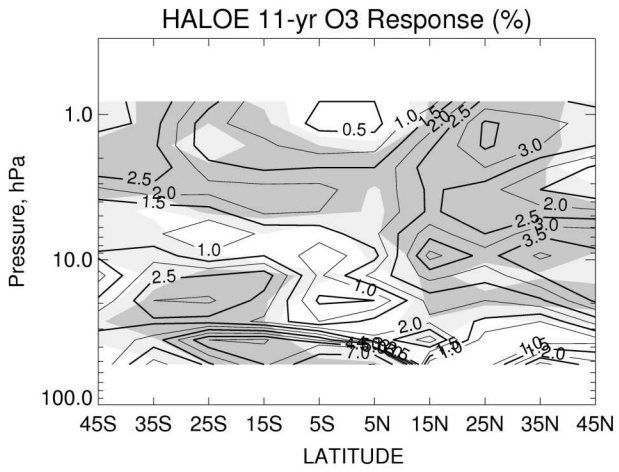

Figure 9. Contour plot of the max minus min 11-yr response (in percent) for HALOE ozone. Contour interval is 0.5% from 0.0 to 5% and is 2% thereafter. Darker shading denotes regions where the response exceeds a CI of 90%; lighter shading has a CI of between 70 and 90%.

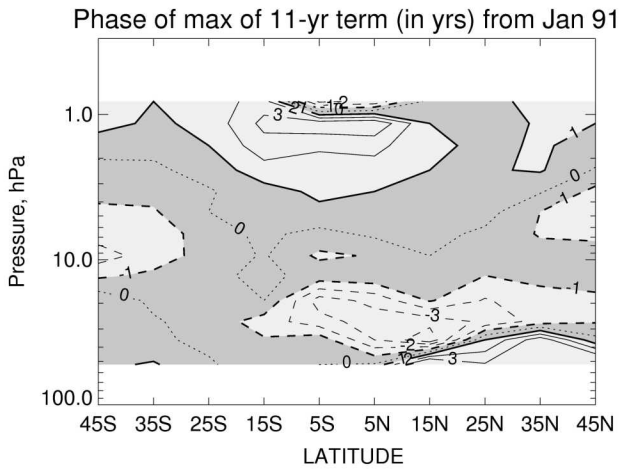

Figure 10. Phase variation of the 11-yr term of Figure 9 (in yrs from January 1991). Contours are: dashed—negative, solid—positive, and dotted—zero, and the interval is 1 yr. The domain within the bold contours of +1 and -1 is considered as in-phase with the SC uv-flux and that region is shaded darker.

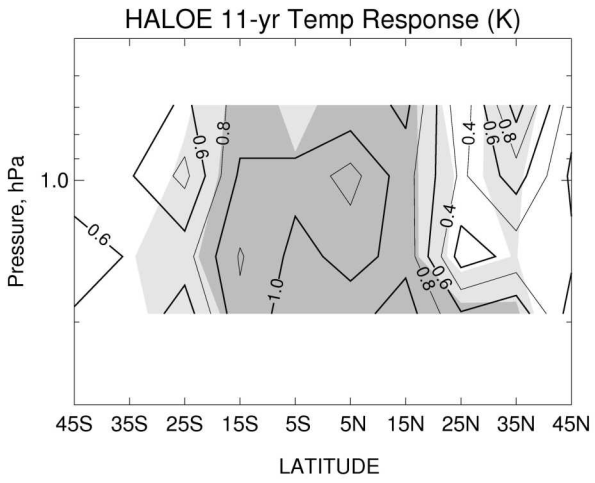

Figure 11. Contour plot of the max minus min 11-yr response (in K) for HALOE temperature. Contour interval is 0.2 K. Darker shading denotes regions where the response exceeds a CI of 90%; lighter shading has a CI of between 70 and 90%.

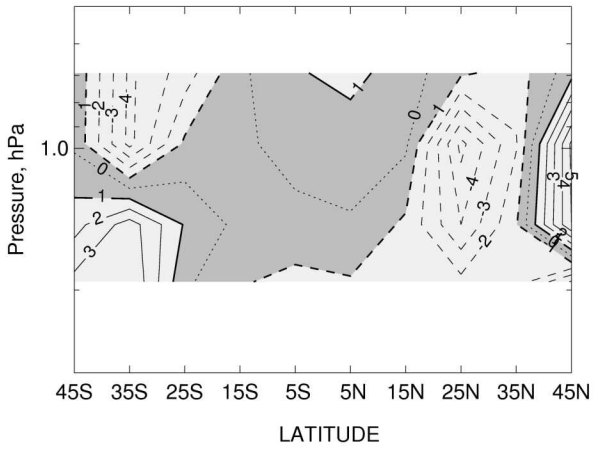

Figure 12. Phase variation of the 11-yr term of Figure 11 (in years from January 1991). Contours are: dashed—negative, solid—positive, and dotted—zero, and the interval is 1 yr. The domain within the bold contours of +1 and -1 is considered as in-phase with the SC uv-flux and that region is shaded darker.

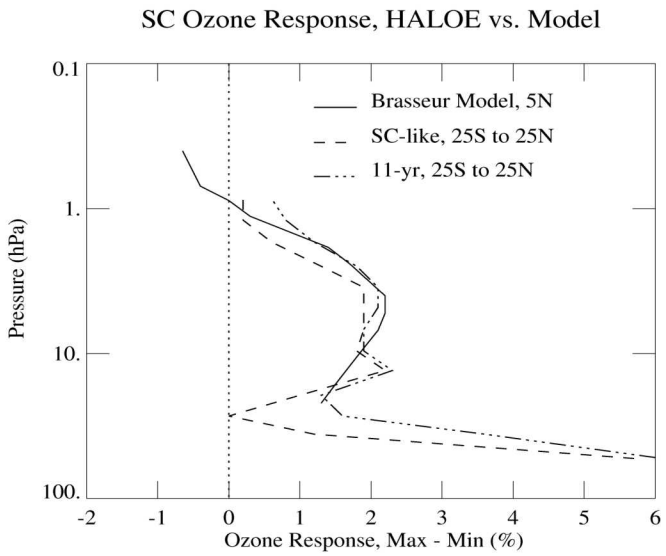

Figure 13. Profiles of the 11-yr and the SC-like, max minus min responses (in percent) for the tropical to subtropical ozone from HALOE. The solid curve is the model result for 5N from *Brasseur* [1993].

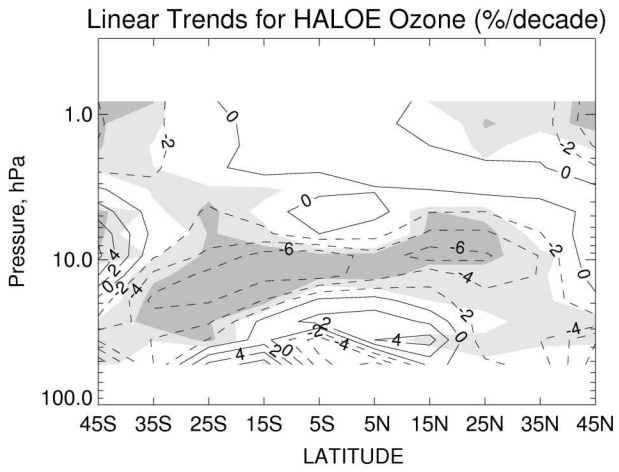

1

2 **Figure 14**. Contour plot of the linear trend terms (in %/decade) from the MLR models of

3 HALOE ozone. Contour interval is 2%; the positive and zero contours are solid, while

4 the negative contours are dashed. Darker shading denotes regions where the trend has a

5 CI exceeding 90%; lighter shading has a CI of between 70 and 90%.